EES Batteries

PAPER

View Article Online
View Journal | View Issue

Cite this: *EES Batteries*, 2025, **1**, 1751

Feasibility studies of acidic type III deep eutectic solvents as supporting electrolytes for the posolyte in vanadium flow batteries

L. Mauricio Murillo-Herrera * and Ana B. Jorge Sobrido

Deep eutectic solvents (DES) are gaining interest as promising electrolytes for vanadium flow batteries due to their tuneable solvation properties, high solubility for ionic species, and their potential green credentials, but their application has been limited to a few formulations, based on ethylene glycol and urea, which are neutral/alkaline DES. Taking into consideration the vanadium redox mechanism in aqueous media, we hypothesized that exploring acidic formulations could improve the redox performance of V(IV/V) posolytes. Here, for the first time, we investigate the effect of binary and tertiary acidic type III DES formulations on the electrochemical kinetics of the V(IV/V) redox couple. Cyclic voltammetry revealed that acidic DES moderately improved anodic performance, but significantly destabilized the cathodic process compared to a neutral hydrogen bond donors, which exhibited better cathodic reversibility. Hydroxyl groups were found to stabilize the cathodic process, likely through coordination to vanadium species, whereas carboxylic acids improved anodic kinetics, but increased cathodic irreversibility. Furthermore, the aqueous dilution of the DES strategy was not found to be universally beneficial since high water loadings were observed to destabilize the redox system. The best performing ternary mixture, consisting of choline chloride, ethylene glycol and malonic acid in 1 : 2 : 2 molar ratio, exhibited a peak-to-peak separation comparable to aqueous acidic electrolytes, but lower operational currents. The improvements were attributed to the balance between pH modulation and viscosity reduction. These new findings highlight the competing effects of viscosity, solvation, speciation and pH on vanadium redox chemistry and provide useful insights on the need to balance these properties to enhance charge transfer and reversibility in the design of DES formulations for flow battery applications.

Received 24th July 2025,
Accepted 20th August 2025

DOI: 10.1039/d5eb00138b

rsc.li/EESBatteries

Broader context

Deep eutectic solvents (DES) have recently emerged as promising electrolytes for flow batteries, offering advantages such as high ionic species solubility, intrinsic ionic conductivity, large electrochemical windows, low toxicity, non-flammability, and task-specificity. Despite their huge molecular flexibility, the application of DES to flow batteries remains narrowed to very few archetypic formulations. Although promising, these electrolytes suffer from high charge transfer and mass transport resistance and overall poor electrochemical performance. Our study explores how modulating DES pH by incorporating carboxylic acid-based formulations, the availability of hydroxyl functional groups, and the mass fraction of the DES components impacts the electrochemical performance of the vanadium(IV/V) redox couple, which is used as the catholyte in vanadium flow batteries. We demonstrate that while organic acids enhance anodic kinetics, they destabilize the cathodic process, whereas polyol-based DES improve cathodic reversibility. Among the ternary formulations studied, certain mixtures exhibited electrochemical reversibility comparable to commercial aqueous vanadium electrolytes, though with lower operational currents, highlighting the challenges of achieving high electrochemical reversibility in DES-based systems. These findings provide valuable insights into how electrolyte composition influences vanadium redox chemistry, which is critical for advancing DES-based flow battery technologies

Introduction

The demand for renewable energy is growing due to increased electrification and a global shift from fossil energy as a response to the climate crisis. The intermittency of solar and wind power requires cost-efficient, reliable and scalable energy storage solutions. Among various technologies, flow batteries have emerged as a promising option due to their high scalability, long cycle life, and capability to decouple energy and power. Vanadium flow batteries are the most commercially developed flow batteries due to their longevity, high reliability, and ease of operation and maintenance.[1,2] The vanadium flow battery stores energy *via* vanadium redox reactions in aqueous

School of Engineering and Materials Science, Queen Mary University of London, Mile End Rd, London E1 4NS, UK. E-mail: l.m.murilloherrera@qmul.ac.uk, a.sobrido@qmul.ac.uk

acidic media, where the anolyte consists of the V(II/III) redox couple and the posolyte the V(IV/V) couple. The advantage of this battery is the use a single transition metal, which eliminates cross-contamination, promoting longer life cycles. However, this technology faces critical challenges including high capital costs, low energy and power densities and sluggish redox kinetics.[2]

In sulfuric acid solution, a coupled electrochemical/chemical mechanism (EC) has been proposed for the V(IV/V) redox process according to reactions (1)–(4). The vanadyl cation undergoes a Nernstian oxidation to VO^{3+} species (1), which is then quickly hydrolyzed to form the dioxovanadium(V) cation VO_2^+ (2). In the reverse process, VO_2^+ undergoes a sluggish reduction to VO_2 (3), followed by reaction with hydronium ions to generate water (4). The modelling of this EC mechanism suggests that transfer coefficients for the overall forward (anodic) and reverse processes are close to 0.5.[3–5]

$$VO^{2+} \rightarrow VO^{3+} + e^- \quad (1)$$

$$VO^{3+} + H_2O \rightarrow VO_2^+ + H_2O + 2H^+ \quad (2)$$

$$VO_2^+ + e^- \rightarrow VO_2 + H_2O + 2H^+ \quad (3)$$

$$VO_2 + 2H^+ \rightarrow VO^{2+} + H_2O \quad (4)$$

Deep eutectic solvents (DES) are mixtures of Brønsted–Lowry or Lewis acids, also known as hydrogen bond donors (HBD), and bases, also known as hydrogen bond acceptors (HBA). These mixtures are characterized by significantly lower melting points than their individual components. Recently, DES have gained attention in energy storage due to their potential for low toxicity, high biodegradability, high metal salt solubility, ionic conductivity, and design flexibility with over 10^6 possible combinations.[6]

One of the key constraints in conventional aqueous electrolytes is the limited solubility of vanadium species, which directly impacts energy storage capacity. DES provide a highly tuneable solvation environment, allowing for enhanced vanadium solubility beyond the limits of traditional sulfuric acid-based systems. Additionally, by carefully designing the solvent composition, it is possible to modulate pH and speciation of the electroactive molecule, to disable side reactions, and to enhance charge transfer kinetics, ultimately leading to higher energy density and improved electrochemical performance.[7]

Type III DES—comprising quaternary ammonium halides and hydrogen bond donors (*e.g.*, polyols, amides, organic acids)—are being explored as electrolytes in batteries, but despite their huge structural flexibility, the application of DES in flow batteries has remained narrowed to mixtures of choline chloride (ChCl) with ethylene glycol, glycerol and urea, the three main archetypes of the DES third type (Fig. 1).[8] The inorganic chemistries studied in type III DES for battery applications were all-Cu,[9] hybrid all-Fe,[10–12] all-V(acac),[13,14] Zn/Ce,[15] Zn-ion[16] and V/Fe.[17–19] All these batteries were demonstrated in static mode, to the best of our knowledge the only DES-based flow battery system was reported by Nayanthara *et al.*

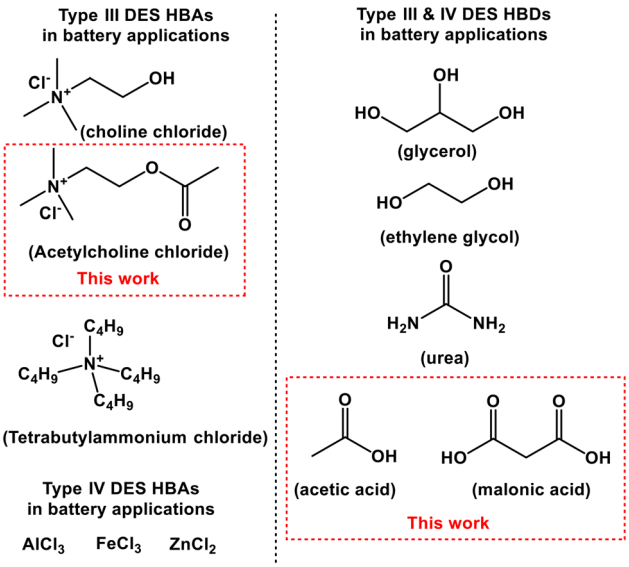

Fig. 1 Type III & IV DES applied to batteries.

using the all-V chemistry type III DES diluted with sulfuric acid and dopped with carbon nanotubes.[20] Type IV DES, typically composed of hydrated metal halides and hydrogen bond donors, have been applied as negolytes in Zn(II)/Zn(0)[21] and Al(III)/Al(0)[21–24] systems, and as posolytes in Fe(II)/Fe(III) systems.[25] Although promising, these electrolytes suffer from high viscosities and low conductivities, which in consequence leads to high cell polarisation resistance, low efficiencies, high pressure drop and low operational currents.

Here we explore for the first time a potential strategy to overcome the kinetic limitations of V(IV/V) posolytes in the archetypical ethylene glycol and urea DES by formulating several acidic type III DES as supporting electrolytes. Since the proposed reaction mechanism in aqueous solution involves proton-transfer steps, we hypothesized that by modulating the pH of the HBD, we enhance the vanadium charge-transfer kinetics. Moreover, ternary mixtures consisting of the base type III DES with water or other HBDs could reduce the electrolytes viscosity and increase the electrochemical performance. Additionally, we postulate that the chloride-rich environment of the DES could stabilizes the V(V) species, which could allow the operation of the posolyte at temperatures above 40 °C, as suggested by previous research on aqueous media.[26–28]

The chosen acidic DES were ChCl/AA (1 : 2) where ChCl is choline chloride and AA acetic acid, ChCl/MA (1 : 1) where MA stands for malonic acid and AcChCl/AA (1 : 2), where AcChCl is acetyl choline chloride. MA is nearly two orders of magnitude stronger acid than AA (pK_a for the first proton-transfer reaction of malonic acid is 2.83 whereas for acetic acid is 4.76), however ChCl/MA (1 : 1) is an order of magnitude more viscous than ChCl/AA (1 : 2).[6,29] Carboxylic acid-based DES can undergo side reactions even at room temperature, such as esterification between carboxylic acid and alcohol-based HBDs or with the alcohol group from the cholinium cation, while MA can

undergo cracking, producing AA even under mild temperatures.[30–32] This irreversible chemical step suggests that ChCl/MA (1 : 1) is not suitable as a supporting electrolyte. However, for the purposes of this investigation, ChCl/MA (1 : 1) provided higher acidity than AA, while being less viscous than other dicarboxylic acid-based DES with similar pK_a, such as oxalic acid or levulinic acid. While the cracking of MA is eventually unavoidable, the esterification reaction is an equilibrium process that can be modulated and potentially leveraged by adjusting the water content in the solvent. For example, a high-throughput analysis of various DES formulations, showed that those based on acetylcholine chloride exhibited higher conductivities than their choline chloride-based counterparts, suggesting that controlled esterification is a valuable strategy to tune DES properties for high performance battery applications.[33]

Materials and methods

Preparation of DES and vanadium electrolytes

All reagents were purchased from Sigma-Aldrich and Fisher chemicals UK. Choline chloride was recrystallised from ethanol, dried under vacuum at room temperature for 24 h and stored in N_2 atmosphere before it was used. The rest of the reagents were used as received. DES were prepared using the heating method. Briefly, the DES components were added to a two-neck round bottom flask under N_2 atmosphere, vigorously stirred at 80 °C until a homogeneous liquid was obtained and stored in a desiccator. The ternary mixtures were prepared by mixing a given DES with x_{mol} = 0.5, 1.0, 2.0 or 4.0 of acetic acid, ethylene glycol or water, *e.g.* ChCl/EG/AA (1 : 2 : 1), thus effectively diluting the HBA. The nomenclature establishes the components of the parent DES in the first two positions from left to right, and the diluting agent in the third position (Table 1).

100 mM solutions of $VOSO_4{\cdot}xH_2O$ (97%, Sigma Aldrich, UK) in each DES sample were prepared. TGA analysis was carried out to determine the water content in the vanadium salt, consistently around 27.5 wt%. $VOSO_4$ did not solubilize in the DES at room temperature. Hence the mixtures were stirred at 60 °C until obtaining homogeneous solutions. The stored solutions remained homogeneous for several months, but eventually precipitation of $VOSO_4$ was observed.

Electrochemical characterization

Cyclic voltammetry (CV) was performed using a water-jacketed three electrode electrochemical cell, equipped with a 3.5 mm glassy carbon disk as working electrode, a Pt coil as counter electrode, BASi leak-free saturated Ag/AgCl reference electrode and a Biologic SP300 potentiostat/galvanostat. The solution resistance was measured using the current-interrupt method and the potentials corrected during data post-processing. The second scan of every CV was used for the data analysis. The glassy carbon disk was manually cleaned in between sample measurements by polishing over a nylon pad with 1 μm diamond polish suspension for 2 minutes and over a velvet pad using a 0.05 μm alumina polishing suspension. Afterwards, the electrode was sonicated in deionized water and ethanol for 5 minutes respectively. The electrode was preconditioned before each measurement by running 20 CV cycles between −1 V and 1.2 V at 50 mV s^{-1} in the corresponding DES.

The transfer coefficients were calculated based on each peak's half-peak-width parameter ($\Delta E_{p-p/2}$) considering irreversible kinetics according to eqn (1), with R the ideal gas constant (J mol^{-1} K^{-1}), T the temperature, a the transfer coefficient and n the number of exchanged electrons, which was assumed as 1.[34] Both CV parameters are reported as the average over all scan rates. The diffusion coefficient of the V(IV/V) species were obtained *via* the irreversible Randles–Ševčík analysis of the i_p *vs.* $\sqrt{v}$ relationship, according to eqn (2), with A the electrode geometric area, C the electroactive species bulk concentration (mol cm^{-3}), D the diffusion constant of the electroactive species (cm^2 s^{-1}) and v the scan rate (A s^{-1}).[34] All i_p *vs.* $\sqrt{v}$ plots and E_p *vs.* log(v) plots used to calculate the peak potential shift rates are displayed in the SI. The heterogeneous rate constant (k_s) was estimated using the Kinglier and Kochi model for irreversible kinetics, which only depends on the peak-to-peak separation (ΔE_p), the transfer coefficient of the forward process and the diffusion coefficient of the species

Table 1 DES labels and corresponding compositions indicated by mass fraction

DES	W_1	W_2	W_3
ChCl/EG (1 : 2)	0.53	0.47	—
ChCl/AA (1 : 2)	0.54	0.46	—
ChCl/MA (1 : 1)	0.57	0.43	—
AcChCl/AA (1 : 2)	0.60	0.40	—
ChCl/EG/H_2O (1 : 2 : 0.5)	0.51	0.46	0.03
ChCl/EG/H_2O (1 : 2 : 1)	0.50	0.44	0.06
ChCl/EG/H_2O (1 : 2 : 2)	0.47	0.41	0.12
ChCl/EG/H_2O (1 : 2 : 4)	0.42	0.37	0.21
ChCl/AA/H_2O (1 : 2 : 0.5)	0.52	0.45	0.03
ChCl/AA/H_2O (1 : 2 : 1)	0.50	0.43	0.07
ChCl/AA/H_2O (1 : 2 : 2)	0.47	0.41	0.12
ChCl/AA/H_2O (1 : 2 : 4)	0.42	0.36	0.22
ChCl/MA/H_2O (1 : 1 : 0.5)	0.55	0.41	0.04
ChCl/MA/H_2O (1 : 1 : 1)	0.53	0.40	0.07
ChCl/MA/H_2O (1 : 1 : 2)	0.50	0.37	0.13
ChCl/MA/H_2O (1 : 1 : 4)	0.44	0.33	0.23
AcChCl/AA/H_2O (1 : 2 : 0.5)	0.58	0.39	0.03
AcChCl/AA/H_2O (1 : 2 : 1)	0.57	0.38	0.06
AcChCl/AA/H_2O (1 : 2 : 2)	0.54	0.36	0.11
AcChCl/AA/H_2O (1 : 2 : 4)	0.49	0.32	0.19
ChCl/EG/AA (1 : 2 : 0.5)	0.48	0.42	0.10
ChCl/EG/AA (1 : 2 : 1)	0.43	0.38	0.19
ChCl/EG/AA (1 : 2 : 2)	0.36	0.32	0.31
ChCl/EG/AA (1 : 2 : 4)	0.28	0.25	0.48
ChCl/AA/EG (1 : 2 : 0.5)	0.48	0.41	0.11
ChCl/AA/EG (1 : 2 : 1)	0.43	0.37	0.19
ChCl/AA/EG (1 : 2 : 2)	0.36	0.31	0.32
ChCl/AA/EG (1 : 2 : 4)	0.27	0.24	0.49
ChCl/MA/EG (1 : 1 : 0.5)	0.51	0.38	0.11
ChCl/MA/EG (1 : 1 : 1)	0.46	0.34	0.20
ChCl/MA/EG (1 : 2 : 2)	0.38	0.28	0.34
ChCl/MA/EG (1 : 2 : 4)	0.28	0.21	0.50
ChCl/EG/MA (1 : 2 : 0.5)	0.44	0.39	0.16
ChCl/EG/MA (1 : 2 : 2)	0.30	0.26	0.44

undergoing the forward process according to eqn (3).[35,36] The reported rate constants represent the average over all scan rates.

$$\Delta E_{p-p/2} = 1.857\frac{RT}{\alpha F} \quad (1)$$

$$i_p = 0.496FAC\sqrt{D}\sqrt{\frac{\alpha Fv}{RT}} \quad (2)$$

$$k^0 = 2.18\sqrt{\frac{aDnvF}{RT}}\exp\left(-\frac{a^2nF}{RT}\right)\Delta E_p \quad (3)$$

The redox properties of the V(IV/V) couple in the ternary mixtures were evaluated using CV. The comparative analysis was performed using the performance metrics obtained at a scan rate of 50 mV s^{-1} as well as the peak shift rates across 5 to 200 mV s^{-1}. Each parameter was normalised between 0 and 1 by scaling to the maximum value obtained for each dilution series and the results represented in radar plots. The CVs from all ternary mixtures between 5 mV s^{-1} to 200 mV s^{-1} is displayed in the SI.

Spectroscopic characterization

The vanadium UV-visible absorption spectra were obtained from 10 mM solutions, using a PerkinElmer Lambda35 UV-vis spectrometer and a Hellma Analytics 1 cm path length quartz cuvette.

Results

Vanadyl speciation in DES

The speciation of the vanadyl electrolyte was studied using UV-vis and FTIR spectroscopy. In sulfuric acid, the vanadyl cation exists as a pentaaquovanadyl(IV) complex $[VO(H_2O)_5]^{2+}$ which is described by an octahedral field (O_h symmetry) compressed due to a Jahn–Teller distortion to a tetragonal C_{4v} symmetry in which the T_{2g} orbitals split into B_2 and E orbitals, whereas the original E_g orbitals split into B_1 and A_1 orbitals.[37] The electronic absorption spectrum of $VOSO_4$ in H_2SO_4, showed a main band at ~760 nm that can be attributed to a B_2 to B_1 transition, whereas the shoulder at ~625 nm can be attributed

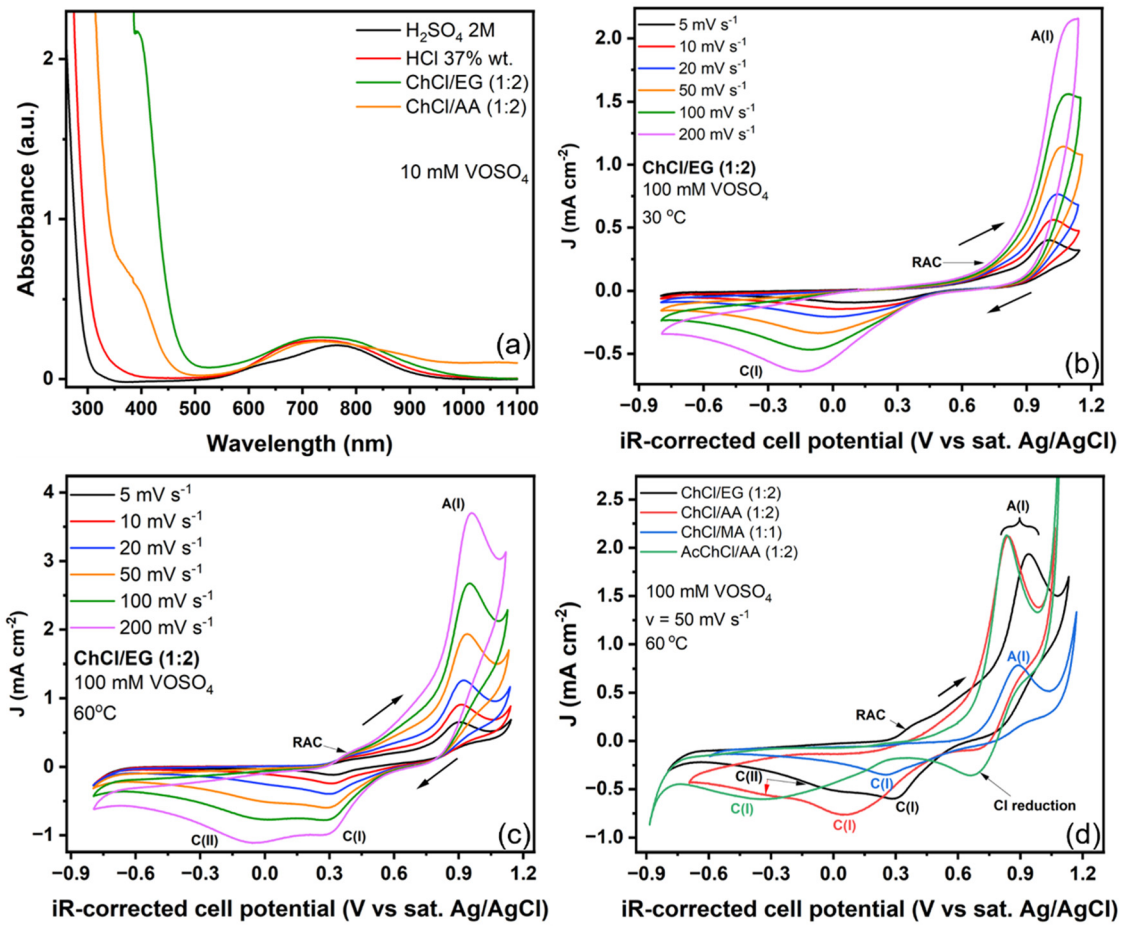

Fig. 2 (a) Spectroscopical characterization of $VOSO_4$ in type III DES: UV-vis spectra of $VOSO_4$ in DES and aqueous solutions. (b) CVs of $VOSO_4$ in ChCl/EG (1 : 2) at 30 °C. (c) CVs of $VOSO_4$ in ChCl/EG (1 : 2) at 60 °C. (d) Comparison of voltammograms from $VOSO_4$ in the studied DES at 60 °C and a scan rate of 50 mV s^{-1}.

to the B_2 to E transition in agreement with the literature (Fig. 2a).[38,39]

Previous spectroscopical characterization of concentrated vanadyl solutions in hydrochloric acid did not reveal significant differences due to chloride coordination to the vanadyl core.[28] However, Furman and Garner reported that it was necessary to increase the concentration of chloride anions in aqueous solution to at least 20 times that of the hexaaquovanadium(III) complex or 100 times the concentration of the pentaaquovanadyl(IV) to observe meaningful changes in the electronic absorption spectrum, thus indicating that the chloride anion marginally coordinates to the vanadyl cation in aqueous solution.[40] Moreover, previous characterization of the $[VOCl_4]^{2-}$ anion in Cl-based ionic liquids identified two bands at 859 and 739 nm associated with B_2 to B_1 and B_2 to E transitions respectively; and two weak extra bands at 430 nm and 364 nm associated with the transition from B_2 to A_1.[41,42] In our experiment, the vanadyl cation was highly diluted with a Cl^- to VO^{2+} ratio of ~1200. In this diluted vanadyl solution, a broad wave centred at 737 nm was observed, likely arising from the convolution of the expected bands. The high energy bands were not detected, probably obscured by the strong charge-transfer absorption and the solvent absorption. The electronic absorption spectra of the vanadyl cation in ChCl/EG (1 : 2) and ChCl/AA (1 : 2) exhibit the same characteristic broad wave centred at 740 nm. The onset of the charge-transfer absorption takes places at lower energy in HCl compared to H_2SO_4 and then again, at lower energy in DES compared to HCl. This is attributed to the lower degree of solvation of the vanadyl complex in DES. Both DES exhibited another wave at 390 to 395 nm. In ChCl/EG (1 : 2), this band was four times more intense than in the case of ChCl/AA (1 : 2). Neither of these features were observed in aqueous solutions of the DES components in a ratio of 7 : 1 with respect the vanadyl cation. In those cases, the spectra resembled that of the sulfuric acid solution. Therefore, the spectroscopical characterization shows that the vanadyl species exists as chlorovanadyl complexes in ChCl-based DES.

Electrochemical characterization of binary mixtures

The electrochemistry of V(IV/V) in ChCl/EG (1 : 2) was studied as a model system for type III DESs at 30 °C and 60 °C (Fig. 2b and c respectively), the voltametric characterization of the binary mixtures is summarized in Table 2.

The V(IV/V) anodic process was characterized by peak A(I) maximum located around 1.04 V in ChCl/EG (1 : 2) at 30 °C (all potentials are reported against the saturated Ag/Ag/Cl electrode) and a peak-to-half-peak width ($\Delta E_{p-p/2}$) value of 91 mV (Table 2, entry 1). At faster scan rates, the peak shifts towards anodic potentials at a rate of 65 mV per decade. The residual anodic current (RAC) increased linearly with the applied overpotential from an onset potential of 0.41 V for $5 < \nu < 50$ mV s^{-1}, which suggests an earlier unresolved irreversible anodic process. The cathodic peak C(I) was characterized by a broader width ($\Delta E_{p-p/2}$ = 206 mV). The onset was observed at around 0.50 V *vs.* Ag/AgCl. The peak centre was observed around 0.05 V *vs.* Ag/AgCl and shifted towards cathodic potentials at faster scan rates at a rate of 179 mV per decade. A shoulder centred around 0.30 V *vs.* Ag/AgCl was detected only at scan rates between 5 and 50 mV s^{-1}, which could indicate that the broadness of the cathodic peak is due to the convolution of two irreversible reduction processes.

The overlap of the supporting electrolyte background CV with the electrolyte containing $VOSO_4$ suggested that the presence of vanadium disfavoured the oxidation of chloride from the solvent. The background CV showed higher anodic and cathodic currents at potentials close to the electrolysis barrier compared to the experiment with vanadium (Fig. S1 in SI). The transfer coefficients of the forward and reverse pathways were not complementary ($\alpha_a + \alpha_c < 1$). The analysis suggested that the merge of C(I) and C(II) generated a convoluted broad wave. Since the calculation of the transfer coefficient depends on the peak $\Delta E_{p-p/2}$ parameter, the convolution of the two peaks resulted in an underestimation of the cathodic transfer coefficient.

The ΔE_p(I) values ranged from 841 mV to 1164 mV between 5 and 200 mV s^{-1}. Therefore, obtaining k_s values in the order of 10^{-9} cm s^{-1}. The Kinglier and Kochi model assumes the

Table 2 Summary of cyclic voltammetry characterization of $VOSO_4$ in DES

Entry	DES	$\frac{dE_{p,a}}{d\log(\nu)}$ (mV dec^{-1})	$\frac{dE_{p,c}}{d\log(\nu)}$ (mV dec^{-1})	$\Delta E_{p,a-p/2}$ (mV)	$\Delta E_{p/2-p,c}$ (mV)	$\frac{\alpha_a}{\alpha_c}$	k_s (cm s^{-1}) × 10^{-8}	$D_{V(V)}$ (cm s^{-2}) × 10^{-8}	$D_{V(V)}$ (cm s^{-2}) × 10^{-8}
1[a]	ChCl/EG (1 : 2)	65 ± 5	179 ± 22	91 ± 5	206 ± 24	0.53 ± 0.03 0.23 ± 0.03	0.23 ± 0.21	0.52 ± 0.06	0.58 ± 0.09
2[b]	ChCl/EG (1 : 2)	33 ± 2	25 ± 7	84 ± 2	130 ± 5	0.63 ± 0.02 0.41 ± 0.02	4.63 ± 1.00	2.27 ± 0.21	0.87 ± 0.08
3[b]	ChCl/AA (1 : 2)	29 ± 2	162 ± 23	82 ± 2	185 ± 18	0.65 ± 0.02 0.29 ± 0.03	1.59 ± 1.63	4.96 ± 0.43	2.17.±0.30
4[b]	ChCl/MA (1 : 1)	51 ± 1	52 ± 2	92 ± 4	162 ± 10	0.58 ± 0.03 0.33 ± 0.02	11.28 ± 0.44	0.83 ± 0.09	0.42 ± 0.05
5[b]	AcChCl/AA (1 : 2)	22 ± 2	329 ± 19	75 ± 4	198 ± 52	0.71 ± 0.03 0.28 ± 0.06	0.03 ± 0.03	5.39 ± 0.53	1.24 ± 0.30

[a] 30 °C. [b] 60 °C.

transfer coefficients are complementary ($\alpha_a + \alpha_c = 1$) and that the peaks related by ΔE_p(I) correspond to the forward and reverse steps of the same redox process. Therefore, the convolution of the cathodic peaks makes the interpretation of the heterogeneous rate constant challenging, because the calculated α_c does not strictly correspond to the reverse process of the V(IV/V) oxidation. Despite the lack of complementarity in the transfer coefficients, the rather small k_s values were consistent with similar systems previously reported in the literature. For context, Pardo *et al.* calculated k_s for the $FeCl_2/FeCl_3$ pair in ChCl/EG (1 : 2) at 25 °C using Pt electrodes obtaining values of $k_s \approx 10^{-7}$ cm s^{-1}.[43] The ΔE_p of their redox process was ~120 mV with a transfer coefficient of 0.57. Since the iron redox process follows a simpler outer-sphere electron transfer mechanism than V(IV/V), it is reasonable for the latter to display k_s that are orders of magnitude lower.

Due to the low water concentration of DES, which is largely committed to the solvent's hydrogen bond network, the VO^{3+} intermediate species generated after the Nernstian oxidation of VO^{2+} likely reacts directly with the alcohols present in the DES, forming a mixture of vanadium(V) chloroalkoxide complexes rather than undergoing hydrolysis.[44] These chemical reactions may contribute to the overall irreversibility of the electrochemical process by rearranging the active V(V) species or by depleting its concentration at the electrode surface due to poorer solvation. This way, the redox reaction would limited by the slowest of the solvolysis reactions, as such the coupling of a second order rate law to the electron-transfer process predicts a peak shift rate of 19.7 mV per decade.[34] However, all the studied anodic processes exhibit larger peak shift rates, suggesting that the EC mechanism alone does not fully account for the irreversibility of the redox process.

The V(V) species can undergo several side reactions. For instance, the reduction of $VOCl_3$ by alcohols and specific carboxylic acids such as propionic or *n*- and iso-butyric acid has been reported in organic solvents, leading to mixtures of chloroalkoxide vanadium complexes.[45]

Dent *et al.* reported that dissolving $VOCl_3$ in 1-ethyl-3-methylimidazolium chloride ionic liquid, resulted in the formation of $[VOCl_4]^{2-}$ instead of $[VOCl_4]^-$ attributed to V(V) deoxochlorination.[42] The same study also reported the disproportionation between $[VO_2Cl_4]^{2-}$ and $[VCl_6]^{3-}$ to obtain $[VOCl_4]^{2-}$.

In chloride-rich aqueous media, at high states of charge, *i.e.*, at near quantitative oxidation to V(V), the Nerst equation predicts a positive shift of the V(IV/V) redox potential, which may promote the reduction of VO_2^+ by chloride anions. However, previous research on highly concentrated aqueous acidic electrolytes have not found substantial deoxochlorination of VO_2^+.[26–28]

In our experiments, the observed RAC is unlikely to originate from the V(III/IV) redox couple. Even if observed at similar redox potentials, this is not commonly seen, due to sluggish electrochemical kinetics. Instead, we attributed this activity to vanadium adducts originating from solvolysis reactions following the anodic process.

Additional experiments were conducted at 60 °C to assess the impact of electrolyte temperature on the electrochemical performance. Previous characterization of the V(II/III) redox couple in DES demonstrated an improvement in electrochemical reversibility and available currents at 55 °C compared to room temperature.[46] Operating vanadyl electrolytes in sulfuric acid at high temperatures is not advised, as dioxovanadium (V) cations dimerize and precipitate above 40 °C.[47] However, it has been reported that chloride anions stabilize V(V), preventing precipitation.[26–28] At higher temperature, the reduction of Cl became more evident, following the DESs anodic oxidation barrier, as a shoulder located at ~0.8 V (Fig. 2c). The cathodic current associated with the reduction of the solvent anodic products varied with the cutoff potential, *i.e.* it depends on how much solvent was electrolyzed.

The temperature increase promoted a nearly threefold improvement of the anodic current peaks and overall positive effect on the anodic process. The anodic peak potential A(I) was observed −70 mV with respect to the peak at 30 °C. The peak shift rate was reduced in ~50% and the $\Delta E_{p-p/2}$ value in ~10% (Table 2, entry 2). RAC was still observed between 0.30 V and 0.75 V. However, this was evident at all scan rates studied, which supports the idea that this current originates from a sluggish vanadium oxidation preceding V(IV/V).

The previously observed broad cathodic wave was resolved into two reduction peaks C(I) and C(II) centred around 0.31 V and −0.03 V respectively. C(I) shifted slightly across the studied scan rates (25 mV per decade), whereas C(II) appeared only as residual current at scan rates below 50 mV s^{-1}. Rising the temperature also promoted a 50% reduction in C(I) peak's $\Delta E_{p-p/2}$ parameter. ΔE_p(I) ranged between 581 mV at 5 mV s^{-1} and 680 mV at 200 mV s^{-1}, which still suggests complete irreversibility, but shows an enhancement compared to 30 °C. The transfer coefficients calculated from each peak's $\Delta E_{p-p/2}$ parameter resulted in ($\alpha_a + \alpha_c \approx 1$). Increasing the temperature had a positive but differentiated effect on the diffusion constant of the V species, showing a fourfold increase for V(IV), but only 50% increase for V(V). Also, the rate constant increased an order of magnitude, driven by the reduction of the ΔE_p parameter. Overall, the vanadyl cation exhibited a complex electrochemistry in ChCl/EG (1 : 2). Naturally, increasing the temperature from 30 °C to 60 °C promoted an increase of the peak currents, lower overpotential and resolved the convoluted cathodic wave into at two clear reduction processes. Based on these observations, the following experiments were conducted at 60 °C. This temperature also provided a more realistic comparison with ChCl/MA (1 : 1), due to its higher viscosity. The voltammograms from the acidic DES at 50 mV s^{-1} are shown in Fig. 2d. A(I) in ChCl/AA (1 : 2) was observed at potentials around 0.830 V and showed ~50% larger currents despite ChCl/AA (1 : 2) being slightly more viscous than ChCl/EG (1 : 2) (70 *vs.* 37 mPa s at 25 °C).[6,29] The anodic peak shift rate and $\Delta E_{p-p/2}$ parameter showed only marginal improvements with respect to ChCl/EG (1 : 2) (Table 2, entry 3). In this case, RAC was also observed at potentials between 0.35 V and 0.66 V. However, this was more noticeable in ChCl/EG (1 : 2).

The cathodic activity of ChCl/AA (1 : 2) was characterized by two processes. Unexpectedly, the onset of reduction was observed at slightly lower potentials than in ChCl/EG (1 : 2) and the first peak was located at potentials around 0.07 V, which translated into larger reduction overpotentials despite the acidity of the solvent. The C(I) shift rate and $\Delta E_{p-p/2}$ parameters also resulted significantly larger than in ChCl/EG (1 : 2). Finally, C(II) was prominent at scan rates above 50 mV s^{-1} similarly as observed for ChCl/EG (1 : 2). Based on the previous metrics, the ΔE_p(I) value ranged from 565 mV at 5 mV s^{-1} to 867 mV at 200 mV s^{-1}, reinforcing the idea that in this DES, the cathodic process was more irreversible than ChCl/EG (1 : 2). The transfer coefficients were close to complementarity ($\alpha_a + \alpha_c \approx 0.95$). The deviation from unity was due to the relatively large cathodic $\Delta E_{p-p/2}$ values. A twofold increase in the diffusion coefficients of V(IV/V) were also observed, which explains the improvements in peak currents. However, a twofold decrease of the rate constant compared to ChCl/EG (1 : 2) was calculated, mainly driven by larger ΔE_p(I) values. The large shift rate of the cathodic peak potential also contributed to the high uncertainty of the rate constant, which was calculated as an average of the rate constant at each scan rate.

The anodic region of the V(IV/V) redox process in ChCl/MA (1 : 1) was characterized only by the A(I) with no traces of RAC at lower potentials. The peak shift rate and the $\Delta E_{p-p/2}$ resulted slightly larger than the previously studied electrolytes at 60 °C, due to the DES high viscosity. The cathodic region exhibited two peaks: C(I) at 0.43 V and C(II) at 0.28 V. C(I) was observed to shift towards more negative potentials at a rate of 51 mV per decade, while C(II) remained relatively constant which caused a merge of both peaks at scan rates above 50 mV s^{-1}, leading to a broadening of the main cathodic peak, with $\Delta E_{p-p/2}$ values comparable with ChCl/AA (1 : 2) (Table 2, entry 4). The V(IV/V) process in ChCl/MA (1 : 1) exhibited ΔE_p(I) values between 540 mV at 5 mV s^{-1} and 683 mV at 200 mV s^{-1}, similarly as observed for ChCl/EG (1 : 2), but the diffusion coefficient values were comparable to those in ChCl/EG (1 : 2) at 30 °C due to the larger viscosity of this DES. The transfer coefficients resulted not close to complementarity ($\alpha_a + \alpha_c \approx 0.91$) due to the cathodic peak broadening. Moreover, the anodic peak $\Delta E_{p-p/2}$ was ~12% larger than the previous DESs, which resulted in a transfer coefficient value of $\alpha_a = 0.58$. Although this value could suggest a more symmetrical potential energy surface (α_a closer to 0.5), the interpretation should be taken with care, as the broadening of the anodic peak could simply be a consequence of the larger viscosity, which would explain why ChCl/EG (1 : 2) at 30 °C also displayed similar transfer coefficient values. Regardless, α_a and ΔE_p(I) were the main promoters of a nearly three-fold increase of the calculated rate constant compared to ChCl/EG (1 : 2) at 60 °C.

Finally, the CVs of the V(IV/V) process in AcChCl/AA (1 : 2) exhibited ~9% larger i_p values than ChCl/AA (1 : 2), whereas the onset of oxidation was observed at practically the same potentials (~0.820 V). The anodic peak shift rate and $\Delta E_{p-p/2}$ parameters were the smallest across the studied DES (Table 2, entry 5). RAC was only observed at scan rates below 20 mV s^{-1}. The cathodic activity was characterized by two peaks C(I) and C(II) centred at $\Delta E_{p,c}$(I) = 0.05 V and $\Delta E_{p,c}$(II) = −0.4 V. C(I) exhibited the largest shift rate across the studied DES, which caused a merge of the two peaks into a single broad peak at faster scan rates, thus exhibiting the largest $\Delta E_{p-p/2}$ across the heated samples as well. The significant cathodic peak shift also promoted the largest ΔE_p(I) values across the studied samples. As discussed in the case of ChCl/EG (1 : 2), since the broad cathodic $\Delta E_{p-p/2}$ value is a consequence of the convolution of two peaks, the derivation of the cathodic transfer coefficient implies an underestimation. As such, the asymmetry of the electrochemical process evidenced by the narrow shape of the anodic peak leads to a fortuitous complementarity of the transfer coefficients ($\alpha_a + \alpha_c \approx 0.99$). As opposed to ChCl/MA (1 : 1), for AcChCl/AA (1 : 2) the rather asymmetric forward transfer coefficient ($\alpha_a \approx 0.71$) and the large ΔE_p(I) values were the main contributors to two orders of magnitude decrease on the estimated rate constant.

Overall, replacing ethylene glycol with acetic acid as HBD improved the peak currents in both redox processes, the diffusion coefficients of V(IV/V) and, to a lesser extent, the kinetics of the anodic process. Unexpectedly, the acidic DES did not show improvements for the V(V) reduction process compared to ChCl/EG (1 : 2), as initially hypothesized. These observations suggest that organic acids had a worse impact on the V(V) reduction process in DES compared to ethylene glycol.

Notably, the worst performing sample was AchChCl/AA (1 : 2), where the alcohol group in the cholinium cation was completely esterified, meaning no alcohol functional groups were involved in the formulation. Therefore, the presence of alcohols resulted more beneficial for the reduction electrochemical kinetics of vanadium than organic acids, although all the redox processes were found to be irreversible. Additionally, the RAC was also more pronounced in ChCl/EG (1 : 2) than in the acidic DES.

Electrochemical characterization of ternary mixtures

The binary mixtures analysis showed that acidic DES had a moderately positive impact on the anodic process of the V(IV/V). However, the cathodic part was significantly destabilised compared to ChCl/EG (1 : 2), which exhibited better cathodic performance. Since dilution is a common strategy to improve the performance of these viscous electrolytes, we analysed whether the addition of water or the HBDs from the binary DES as diluting agents could enhance V(IV/V) electrochemical kinetics.[43,48]

The addition of water led to notable improvements in electrochemical performance, primarily by reducing viscosity, increasing current densities, and lowering overpotentials. However, the extent of these benefits varied depending on the composition of the DES and the water content. The best performing samples from each set of ternary DES mixtures are displayed in Fig. 3.

Moderate water contents ($x_{H_2O} < 2.0$) improved the cathodic process by decreasing peak overpotentials and peak widths, while also enhancing current densities. However, higher water

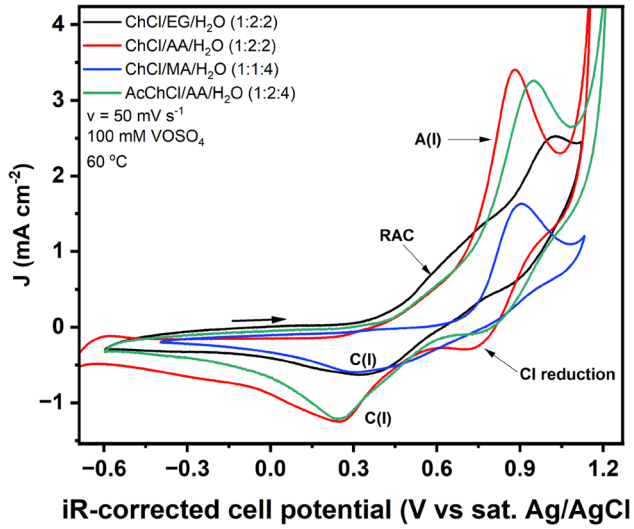

Fig. 3 Representative $VOSO_4$ CVs in DES diluted with water.

contents (x_{H_2O} = 4.0) often resulted in an overall destabilization of the redox process, leading to larger peak separations and increased cathodic shift rates. This suggests that while reducing viscosity facilitates charge transfer, excessive dilution may disrupt stabilizing interactions with vanadium, such chloride coordination or specific hydrogen bonding interactions, which would promote better solvation. Interestingly, in the case of AcChCl/AA (1 : 2), which lacks alcohol functional groups, water addition significantly improved cathodic stability, likely due to the hydrolysis of acetylcholine chloride, leading to acetate anions influencing the redox environment. Despite these improvements, the V(IV/V) redox process remained fully irreversible across all studied systems. As an example, the lowest ΔE_p(I) value obtained was 410 mV for the ChCl/EG/H_2O (1 : 2 : 0.5) mixture, with the cost of lower available currents than its more diluted counterparts. The full analysis is provided in the SI and displayed in Fig. S42.

The voltammetric experiments performed on ChCl/EG/AA (1 : x : y) mixtures showed mixed performance trends depending on the base DES used. CVs obtained from ChCl/EG/AA (1 : 2 : 2) ternary mixtures based on ChCl/EG (1 : 2) exhibited different features compared to those arising from ChCl/AA (1 : 2). We attributed these observations to differences in the water content and the degree of esterification of the base DESs. For clarity, the electrochemical performance metrics and the CVs corresponding to the ChCl/EG (1 : 2)-based and ChCl/AA (1 : 2)-based mixtures are displayed separately in Fig. S59.

Overall, in agreement with the previous binary mixture's characterization, better anodic performance was correlated with higher acetic acid content, whereas higher ethylene glycol fractions resulted better for stabilizing the cathodic process. Lower fractions of choline chloride also resulted in performance increases, thus underscoring the benefits of diluting the DES. The best performing sample of the ChCl/EG/AA (1 : x : y) group of mixtures resulted ChCl/EG/AA (1 : 2 : 2), as it was the sample exhibiting the smallest ΔE_p(I) (0.576 V), the second largest peak currents and shorter anodic and cathodic $\Delta E_{p-p/2}$ widths than the corresponding binary supporting electrolytes. However, as found for the ternary mixtures, vanadium follows completely irreversible electrochemical kinetics. The full analysis is provided in the SI.

The ChCl/MA/EG (1 : x : y) set resulted the best performing of the studied ternary mixtures in terms of the ΔE_p(I) parameter, which resulted similar to those observed in aqueous acidic solutions.[49] A summary of the CV metrics and voltammograms is displayed in Fig. 4. The anodic region of these CVs was characterised only by one peak A(I) at potentials between 0.85 V and 0.94 V. As observed for the ChCl/MA (1 : 1) binary mixtures, no RAC was detected even when using high ethylene glycol content. The cathodic region of the CVs was characterised by only one reduction peak C(I) at potentials between 0.25 V and 0.53 V. Unlike ChCl/EG (1 : 2), the ternary mixtures did not show any peaks at potentials were C(II) was observed, regardless of the amount of ethylene glycol employed (Fig. 4a).

Some correlations were identified between the mass fractions of the diluting agents ($w_{component}$) and the CV performance metrics. However, these were challenging to disentangle since electrochemical performance depends on multiple factors, including viscosity, pH, ion coordination and vanadium interaction with specific functional groups, that are also interconnected (Fig. 4b). For example, malonic acid reduces the solution pH but increases its viscosity.

The ChCl/MA/EG (1 : x : y) electrolytes promoted the smallest ΔE_p(I) values of this work. The improvements compared to the parent DES were explained by an overpotential reduction of both anodic and cathodic processes, with ChCl/MA/EG (1 : 2 : 2) exhibiting ΔE_p(I) = 327 mV. It is important to note that although these metrics reflect differences in redox kinetics amongst the different formulations, the analysis is not intended to predict full-cell performance, but rather to identify electrolyte composition trends that promote the most favourable environments for V(IV/V) redox reactions.

Higher w_{ChCl} and w_{EG} values generally led to increasing anodic peak potentials. Conversely, intermediate to large w_{MA} correlated with lower anodic overpotentials. As such, ChCl/EG (1 : 2) (w_{ChCl} = 0.53, w_{EG} = 0.47) exhibited the largest anodic overpotential, whereas ChCl/MA/EG (1 : 0.5 : 2) (w_{ChCl} = 0.44, w_{MA} = 0.17, w_{EG} = 0.39) and ChCl/MA/EG (1 : 2 : 2) (w_{ChCl} = 0.30, w_{MA} = 0.44, w_{EG} = 0.26) resulted in the lowest. On the other hand, smaller cathodic peak overpotentials loosely correlated with higher w_{MA} and w_{EG} and consequently lower w_{ChCl}. Therefore, ChCl/MA/EG (1 : 2 : 2) exhibited the lowest cathodic overpotential.

The analysis of the binary mixture showed that the acid moderately contributed to the stabilisation of the anodic process when comparing polyol-based DES against organic acid-based DES, which is in line with the ternary mixture's findings. This suggests that the A(I) peak potential stabilization mostly depended on the pH. Naturally, the fact that higher overpotentials were correlated with higher ChCl contents indicates that the anodic process was negatively impacted

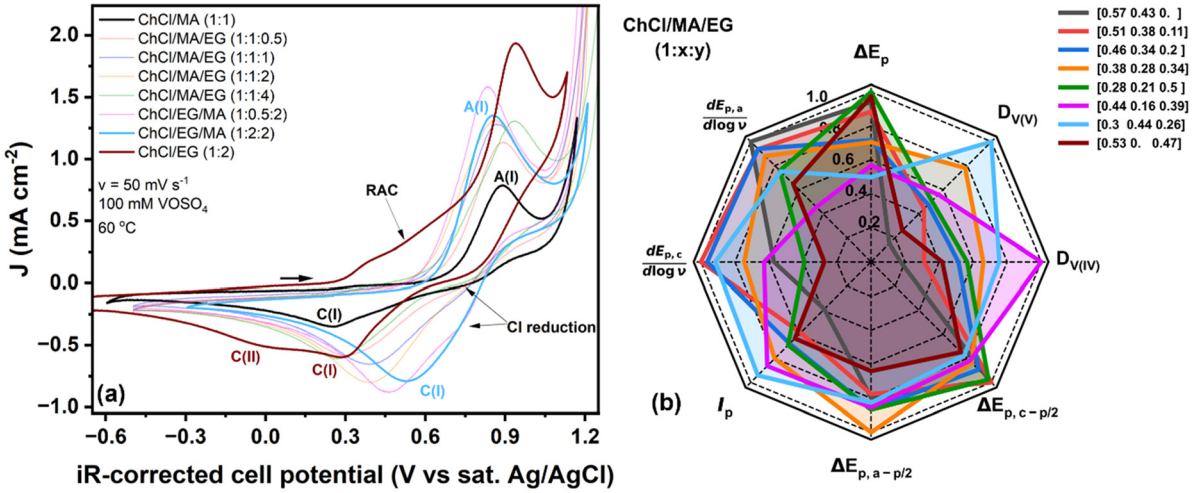

Fig. 4 Electrochemical analysis of ternary mixtures based on ChCl MA and EG. (a) CVs highlighting the parent DES and the ternary mixture with the most reversible kinetics at 60 °C and 50 mV s^{-1}: ChCl/EG/MA (1 : 2 : 2). (b) Radar plot of electrochemical metrics extracted from CVs across the ternary mixtures expressed as mass fractions.

by the viscosity. Conversely, the presence of alcohol functionalities as in ChCl/EG (1 : 2) were observed to stabilize the cathodic process, whereas the organic acids had an opposite effect. In this case, an improvement arising from the combination of malonic acid and ethylene glycol was evident, compared to the parent DESs.

The anodic $\Delta E_{p-p/2}$ width, was correlated with higher w_{ChCl} and correspondingly, with lower w_{MA} values. On the other hand, no trends between this parameter and w_{EG} were observed. Therefore, A(I) peak width appeared most affected by the concentration of chloride, whereas viscosity and pH had a lower impact. This way, ChCl/MA (1 : 1) and ChCl/MA/EG (1 : 1 : 0.5) promoted the shortest anodic peak widths. The shift for the A(I) peak potential at faster scan rates decreased with decreasing lower w_{MA} and w_{ChCl} and increasing w_{EG}. Therefore, the lowest observed anodic shift rates corresponded to ChCl/MA/EG (1 : 0.5 : 2) and ChCl/EG (1 : 2), which suggest that changes in viscosity/conductivity are mostly responsible for the variation in peak shift rate.

Shorter C(I) $\Delta E_{p-p/2}$ widths and lower peak potential shift rates were correlated with higher w_{EG}, and lower w_{MA}, whereas w_{ChCl} had relatively little influence in the variations of these parameters despite the increased viscosity associated with high ChCl contents. Even though there was a correlation between the cathodic peak potential and higher fractions of malonic acid, its presence was observed to increase C(I) shift rate and width, indicating an overall destabilisation of the cathodic process, as observed in the binary mixture analysis. Therefore, ChCl/EG (1 : 2) exhibited the best performance according to these metrics.

As expected, larger V(IV) diffusion coefficients and in consequence, larger anodic currents, were obtained in correlation with lower w_{ChCl} and w_{MA} and larger w_{EG}. However, the largest values were observed for ChCl/MA/EG (1 : 0.5 : 2) and (1 : 2 : 2) instead of ChCl/EG (1 : 2). This is attributed to the significant RAC in the parent binary DES. Since the current was measured from the onset of the main peak, the segment corresponding to the RAC was not considered. The C(I) peak current and the calculated diffusion coefficient were equally observed to correlate with lower w_{ChCl} and larger w_{EG} and to a lesser extent with larger w_{MA}. The contribution of w_{MA} was attributed to the fact that malonic acid discouraged the process associated with C(II), which consequently increased the maximum cathodic currents in all the studied ternary mixtures.

Conclusions

The electrochemical properties of the V(IV/V) redox couple, widely used as a posolyte material in all-vanadium redox flow batteries, were characterized using four different DES: ChCl/EG (1 : 2), ChCl/AA (1 : 2), ChCl/MA (1 : 1), and AcChCl/AA (1 : 2). The addition of water was also explored in ternary mixtures. A comparative analysis of polyol-based DES *versus* acid-based DES revealed that organic acids moderately stabilized the anodic process. However, they led to a significant destabilization of the cathodic process. This was evidenced by larger peak overpotentials and increased cathodic peak shift rates at faster scan rates. This was significantly distinct for AcChCl/AA (1 : 2), where the absence of ethylene glycol and the full esterification of the cholinium cation's alcohol group resulted in the largest cathodic peak separation and the poorest performance. Unexpectedly, these findings suggest that the alcohol groups are responsible for the stabilization of the cathodic process, rather than the organic acids. This stabilization is possibly achieved through alkoxy coordination to the vanadium centre, similarly as the hydrolysis mechanism proposed for the V(IV/V) couple in aqueous acidic media. The V(IV/V) redox process remained fully irreversible across all the binary DES electrolytes, with peak-to-peak separations ranging

from 600 to 1100 mV, corresponding to heterogeneous rate constants on the order of 10^{-8} cm s^{-1}. The comparative electrochemical metrics clearly indicate the more challenging nature of the cathodic process compared to the anodic one, that exhibited larger overpotentials, broader peaks, and higher peak shift rates.

The electrochemical properties of the V(IV/V) redox couple were evaluated in ternary mixtures formulated by diluting ChCl/EG (1 : 2), ChCl/AA (1 : 2), AcChCl/AA (1 : 2) and ChCl/MA (1 : 1) with water, ethylene glycol, or acetic acid. Dilution with water improved the cathodic performance by reducing peak-to-peak potential differences in up to 35%, and cathodic peak widths at low water contents. However, at higher water contents *e.g.* x_{H_2O} = 4.0, an overall destabilization of the redox process was observed, as suggested by increased peak overpotentials, cathodic peak shift rates, and broader cathodic peaks. This indicates that, while a moderate amount of water enhances mass transport and lowers viscosity, excessive amounts of water negatively impact the redox stability, likely due to pH modulation or disruption of stabilizing interactions.

Across all compositions of ChCl/EG/AA and ChCl/AA/EG mixtures, the inclusion of acetic acid led to a progressive reduction in viscosity, which in turn facilitated mass transport and resulted in higher anodic peak currents and lower overpotentials. Higher contents of acetic acid showed only moderate improvements in the anodic peak reversibility. However, increasing content also led to a gradual destabilisation of the cathodic process, as evidenced by larger peak separations, higher cathodic peak shift rates, and, in some cases, the emergence of additional cathodic features. Conversely, mixtures with a higher fraction of ethylene glycol exhibited a more balanced electrochemical response, where the cathodic process was comparatively more stable, although still irreversible. This was reflected in lower peak shift rates at faster scan rates. The opposing effects of these two components highlight the competing influences of viscosity reduction (favouring mass transport) and solvation interactions (governing redox stability) in DES-based electrolytes. An increase in malonic acid content led to a progressive stabilisation of the anodic process, reducing the RAC and minimizing anodic peak broadening. This effect suggests that malonic acid plays a role in stabilizing the oxidized vanadium species, potentially through specific solvation or coordination interactions. However, increasing malonic acid concentration also led to a slight increase in cathodic overpotentials, indicating that while the anodic step benefited from the presence of carboxyl groups, the cathodic reduction of V(V) to V(IV) remained kinetically hindered. A higher ethylene glycol content, in contrast, contributed to a more balanced electron transfer process, improving cathodic stability while still preserving moderate anodic stabilization. This was reflected in lower peak shift rates, suggesting that glycol-rich compositions provided a more favourable solvation environment for vanadium species in both oxidation and reduction. The most optimized behaviour was observed in ChCl/MA/EG (1 : 2 : 2), which exhibited peak-to-peak separations comparable to those observed in aqueous acidic electrolytes, moderate cathodic overpotentials, and a well-defined anodic/cathodic response.

These results highlight the complex interplay between viscosity, solvation structure, and electrochemical kinetics, emphasizing that reducing viscosity alone is insufficient to achieve full redox reversibility in DES-based electrolytes. This work also emphasizes the importance of the DES composition to design systems with optimized mass transport, solvation effects, and kinetic barriers in the V(IV/V) redox process. Despite improvements in specific electrochemical parameters, the V(IV/V) process remained fully irreversible across all studied systems, reinforcing the need for further molecular engineering of DES electrolytes to reduce viscosity and enhance charge transfer kinetics and redox stability for vanadium redox flow battery applications. As such, future work could explore alternative HBA anions, complexing agents, or additional additives to further improve charge transfer rates and reversibility in DES-based electrolytes.

Author contributions

A. B. J. S.: conceptualization, writing – review & editing, funding acquisition. L. M. M. H.: conceptualization, data acquisition & curation, writing – original draft.

Conflicts of interest

The authors declare that there are no conflicts of interest.

Data availability

All processed cyclic voltammetry data as well as current *vs.* square root of the scan rate plots, potential *vs.* the logarithm of the scan rate plots and the analysis of the ternary mixtures with water are displayed in the SI. Raw cyclic voltammetry data and electronic absorption spectra can be provided upon request.

Supplementary information is available. See DOI: https://doi.org/10.1039/d5eb00138b.

Acknowledgements

A. B. J. S. acknowledges the UK Research and Innovation for Future Leaders Fellowship no. MR/T041412/1.

References

1 K. E. Rodby, T. J. Carney, Y. A. Gandomi, J. L. Barton, R. M. Darling and F. R. Brushett, *J. Power Sources*, 2020, **460**, 227958–227969.
2 M. Skyllas-Kazacos, L. Cao, M. Kazacos, N. Kausar and A. Mousa, *ChemSusChem*, 2016, **9**, 1521–1543.

3 J. Lee, J. T. Muya, H. Chung and J. Chang, *ACS Appl. Mater. Interfaces*, 2019, **11**, 42066–42077.
4 M. Gattrell, J. Park, B. MacDougall, J. Apte, S. McCarthy and C. W. Wu, *J. Electrochem. Soc.*, 2004, **151**, A123–A130.
5 M. Gattrell, J. Qian, C. Stewart, P. Graham and B. Macdougall, *Electrochim. Acta*, 2005, **51**, 395–407.
6 K. De Oliveira Vigier and F. Jérôme, in *Deep Eutectic Solvents: Synthesis, Properties and Applications*, ed. D. J. Ramón and G. Guilleana, Wiley-CH, Germany, 2021, ch. 1, pp. 1–21.
7 A. Sharma, R. Sharma, R. C. Thakur and L. Singh, *J. Energy Chem.*, 2023, **82**, 592–626.
8 Y. Ji, H. Zhou, P. Sun, J. Liu, Q. Li, P. Lu and Q. Xu, *Int. J. Green Energy*, 2022, 1–11.
9 D. Lloyd, T. Vainikka and K. Kontturi, *Electrochim. Acta*, 2013, **100**, 18–23.
10 D. Lloyd, V. Toumas, M. Ronkainen and K. Kontturi, *Electrochim. Acta*, 2013, **109**, 843–851.
11 M. A. Miller, J. S. Wainright and R. F. Savinell, *J. Electrochem. Soc.*, 2017, **164**, A796–A803.
12 X. Cheng, T. Xuan and L. Wang, *Chem. Eng. J.*, 2024, **491**, 151936.
13 L. Bahadori, M. A. Hashim, N. S. A. Manan, F. S. Mjalli, I. M. Alnashef, N. P. Brandon and M. H. Chakrabarti, *J. Electrochem. Soc.*, 2016, **163**, A632–A638.
14 B. Chakrabarti, J. Rubio-Garcia, E. Kalamaras, V. Yufit, F. Tariq, C. T. J. Low, A. Kucernak and N. Brandon, *Batteries*, 2020, **6**, 38.
15 X. Cao, S. Wang and X. Xue, *ChemSusChem*, 2021, **14**, 1747–1755.
16 W. Kao-Ian, R. Pornprasertsuk, P. Thamyongkit, T. Maiyalagan and S. Kheawhom, *J. Electrochem. Soc.*, 2019, **166**, A1063–A1069.
17 Q. Xu, L. Y. Qin, Y. N. Ji, P. K. Leung, H. N. Su, F. Qiao, W. W. Yang, A. A. Shah and H. M. Li, *Electrochim. Acta*, 2019, **293**, 426–431.
18 L. Zhao, Q. Ma, Q. Xu, H. Su and W. Zhang, *Ionics*, 2021, **27**, 4315–4325.
19 R. Cheng, J. Xu, J. Zhang, P. Leung, Q. Ma, H. Su, W. Yang and Q. Xu, *J. Power Sources*, 2021, **483**, 1–7.
20 P. S. Nayanthara, S. Sreenath, V. Dave, P. Kumar, V. Verma and R. Nagarale, *Electrochim. Acta*, 2024, **508**, 145242.
21 Y. Wang, Z. Niu, Q. Zheng, C. Zhang, J. Ye, G. Dai, Y. Zhao and X. Zhang, *Sci. Rep.*, 2018, **8**, 5740.
22 M. Angell, C.-J. Pan, Y. Rong, C. Yuan, M.-C. Lin, B.-J. Hwang and H. Dai, *Proc. Natl. Acad. Sci. U. S. A.*, 2017, **114**, 834–839.
23 L. Zhang, C. Zhang, Y. Ding, K. Ramirez-Meyers and G. Yu, *Joule*, 2017, **1**, 623–633.
24 C. Zhang, Y. Ding, L. Zhang, X. Wang, Y. Zhao, X. Zhang and G. Yu, *Angew. Chem., Int. Ed.*, 2017, **56**, 7454–7459.
25 Y. Wang and H. Zhou, *Energy Environ. Sci.*, 2016, **9**, 2267–2272.
26 L. Li, S. Kim, W. Wang, M. Vijayakumar, Z. Nie, B. Chen, J. Zhang, G. Xia, J. Hu, G. Graff, J. Liu and Z. Yang, *Adv. Energy Mater.*, 2011, **1**, 394–400.
27 S. Kim, M. Vijayakumar, W. Wang, J. Zhang, B. Chen, Z. Nie, F. Chen, J. Hu, L. Li and Z. Yang, *Phys. Chem. Chem. Phys.*, 2011, **13**, 18186.
28 N. Roznyatovskaya, J. Noack, H. Mild, M. Fühl, P. Fischer, K. Pinkwart, J. Tübke and M. Skyllas-Kazacos, *Batteries*, 2019, **5**, 13.
29 D. Połomski and M. Chotkowski, *J. Solid State Electrochem.*, 2023, **28**, 1463–1474.
30 M. R. Pinho, A. S. Lima, G. d. A. R. Oliveira, L. M. Liao, E. Franceschi, R. da Silva and L. Cardozo-Filho, *J. Chem. Eng. Data*, 2024, **69**, 3403–3414.
31 R. S. B. Ferreira, A. M. Ferreira, J. A. P. Coutinho and E. A. C. Batista, *ACS Sustainable Chem. Eng.*, 2024, **12**, 15893–15900.
32 N. Rodriguez Rodriguez, A. van den Bruinhorst, L. J. B. M. Kollau and K. Binnemans, *ACS Sustainable Chem. Eng.*, 2019, **7**, 11521–11528.
33 J. Rodriguez, M. Politi, S. Adler, D. Beck and L. Pozzo, *Mol. Syst. Des. Eng.*, 2022, **7**, 933–949.
34 J.-M. Savéant and C. Costentin, *Elements of Molecular and Biomolecular Electrochemistry*, Wiley, 2nd edn, 2019.
35 M. G. Trachioti, A. C. Lazanas and M. I. Prodromidis, *Microchim. Acta*, 2023, **190**, 251.
36 R. J. Klingler and J. K. Kochi, *J. Phys. Chem.*, 1981, **85**, 1731–1741.
37 C. J. Ballhausen and H. B. Gray, *Inorg. Chem.*, 1962, **1**, 111–122.
38 P. Loktionov, R. Pichugov, D. Konev, M. Petrov, A. Pustovalova and A. Antipov, *J. Electroanal. Chem.*, 2022, **925**, 116912.
39 R. P. Brooker, C. J. Bell, L. J. Bonville, H. R. Kunz and J. M. Fenton, *J. Electrochem. Soc.*, 2015, **162**, A608–A613.
40 S. C. Furman and C. S. Garner, *J. Am. Chem. Soc.*, 1950, **72**, 1785–1789.
41 P. B. Hitchcock, R. J. Lewis and T. Welton, *Polyhedron*, 1993, **12**, 2039–2044.
42 A. J. Dent, A. Lees, R. J. Lewis and T. Welton, *J. Chem. Soc., Dalton Trans.*, 1996, 2787–2792.
43 M. D. Pardo, X. Shen, R. F. Savinell and C. Burda, *Electrochim. Acta*, 2023, **467**, 143082.
44 J. Selbin, *Chem. Rev.*, 1965, **65**, 153–175.
45 D. Nicholls, *Coord. Chem. Rev.*, 1966, **1**, 379–414.
46 Q. Xu, L. Y. Qin, H. N. Su, L. Xu, P. K. Leung, C. Yang and H. Li, *J. Energy Eng.*, 2017, **143**, 04017051.
47 M. Skyllas-Kazacos, C. Menictas and M. Kazacos, *J. Electrochem. Soc.*, 1996, **143**, L86–L88.
48 W. Dean, M. Muñoz, N. Juran, Y. Liang, W. Wang and B. Gurkan, *Electrochim. Acta*, 2024, **474**, 143517.
49 J. S. Lawton, S. M. Tiano, D. J. Donnelly, S. P. Flanagan and T. M. Arruda, *Batteries*, 2018, **4**, 40.